Multiparametric Magnetic Resonance Imaging for Discriminating Low-Grade From High-Grade Prostate Cancer

Eline K. Vos, MD, Thiele Kobus, PhD,* Geert J.S. Litjens, PhD,* Thomas Hambrock, MD, PhD,* Christina A. Hulsbergen-van de Kaa, MD, PhD,† Jelle O. Barentsz, MD, PhD,* Marnix C. Maas, PhD,* and Tom W.J. Scheenen, PhD**

Objective: The aim of this study was to determine and validate the optimal combination of parameters derived from 3-T diffusion-weighted imaging, dynamic contrast-enhanced imaging, and magnetic resonance (MR) spectroscopic imaging for discriminating low-grade from high-grade prostate cancer (PCa).

Materials and Methods: The study was approved by the institutional review board, and the need for informed consent was waived. Ninety-four patients with PCa who had undergone multiparametric MR imaging (MRI) before prostatectomy were included. Cancer was indicated on T2-weighted images, blinded to any functional data, with prostatectomy specimens as the reference standard. Tumors were classified as low grade or high grade based on Gleason score; peripheral zone (PZ) and transition zone (TZ) tumors were analyzed separately. In a development set (43 patients), the optimal combination of multiparametric MRI parameters was determined using logistic regression modeling. Subsequently, this combination was evaluated in a separate validation set (51 patients).

Results: In the PZ, the 25th percentile of apparent diffusion coefficient (ADC) derived from diffusion-weighted imaging and washout (WO25) derived from dynamic contrast-enhanced MRI offered the optimal combination of parameters. In the TZ, WO25 and the choline over spermine + creatine ratio (C/SC) derived from MR spectroscopic imaging showed the highest discriminating performance. Using the models built with the development set, 48 (74%) of 65 cancer lesions were classified correctly in the validation set.

Conclusions: Multiparametric MRI is a useful tool for the discrimination between low-grade and high-grade PCa and performs better than any individual functional parameter in both the PZ and TZ. The 25th percentile of ADC + WO25 offered the optimal combination in the PZ, and the choline over spermine + creatine ratio + WO25 offered the optimal combination in the TZ. The ADC parameter has no additional value for the assessment of PCa aggressiveness in the TZ.

Key Words: prostate cancer, prostate cancer aggressiveness, multiparametric MRI, diffusion-weighted imaging, dynamic contrast-enhanced imaging, MR spectroscopic imaging

(*Invest Radiol* 2015;00: 00–00)

Magnetic resonance imaging (MRI) is an emerging technique for the diagnosis and management of prostate cancer (PCa). T2-weighted imaging (T2WI) enables good visualization of morphology and anatomical details, whereas other techniques can provide additional functional information; diffusion-weighted imaging (DWI) represents motion and restriction of water molecules, dynamic contrast-enhanced (DCE) MRI provides information about perfusion and vascular permeability of prostate tissue, and MR spectroscopic imaging (MRSI) gives insight in tissue metabolism. Combining these techniques is commonly referred to as multiparametric MRI (mpMRI), and it is increasingly used for detection and localization of suspicious lesions within the prostate.[1–6]

After detection, an accurate assessment of aggressiveness is of crucial importance, as a substantial proportion of all PCa is considered indolent.[7,8] Current clinical tools such as systematic transrectal ultrasound biopsies often fail to accurately characterize the disease and do not always include anterior sampling of the prostate.[9,10] This increases the risk for underestimation of the disease. Current overtreatment of indolent PCa is an unfortunate consequence of lack of trust in assessment of aggressiveness. Development of more accurate diagnostic and surveillance tools will improve the selection of treatment options, enabling the urologist to discriminate patients suitable for active surveillance from those who need immediate radical treatment.[11]

Currently, MRI is gaining interest for the assessment of aggressiveness of PCa. Several studies have shown that DWI,[12–15] DCE-MRI,[16] and MRSI[17] have potential to achieve this. Despite promising results, substantial overlap existed between different aggressiveness levels, hampering the use of single functional parameters to separate between aggressiveness classes on an individual patient basis. Alternatively, few studies have explored the additional value of combining 2 techniques[18,19] and did not describe the predictive performance. Moreover, an evaluation of all 3 functional techniques to determine the optimal combination to predict PCa aggressiveness has not been carried out thus far.

Therefore, the purpose of this study was 2-fold—determining the optimal combination of functional parameters derived from DWI, DCE-MRI, and MRSI in an mpMRI setting to discriminate between low-grade and high-grade PCa, followed by a validation study to confirm its value.

MATERIALS AND METHODS

Patient Characteristics

The institutional review board waived the need for informed consent. Between 2007 and 2013, all patients who had undergone a full mpMRI protocol (including all 3 techniques—DWI, DCE-MRI, and MRSI) before radical prostatectomy were enrolled in the study. Exclusion criteria were examinations with a combination of only 2 of the functional imaging techniques, previous therapy for PCa (eg, radiotherapy, hormonal therapy), and the usual contraindications for MRI (eg, cardiac pacemaker).

One hundred nine patients were included. Of these, the first 51 subjects scanned between 2007 and 2009 were assigned to the development set used to determine a model with a combination of parameters that best reflects PCa aggressiveness. The remaining 58 subjects scanned between 2010 and 2013 were enrolled in a separate validation set to test the model (Fig. 1).

Received for publication October 28, 2014; and accepted for publication, after revision, February 24, 2015.

From the Departments of *Radiology and Nuclear Medicine, and †Pathology, Radboud University Medical Center, Nijmegen, the Netherlands.

Conflicts of interest and sources of funding: This work received funding from the European Research Council (FP7/2007-2013)/ERC grant agreement 243115 and was also supported by a program grant from the Dutch Cancer Society (KWF: KUN 2007/3971), which both had no role in the performance or reporting of the study.

The authors report no conflicts of interest.

Reprints: Eline K. Vos, MD, Department of Radiology and Nuclear Medicine, Radboud University Medical Center, Geert Grooteplein 10, PO Box 9101, 6500 HB, Nijmegen, the Netherlands. E-mail: eline.vos@radboudumc.nl.

ISSN: 0020-9996/15/0000–0000

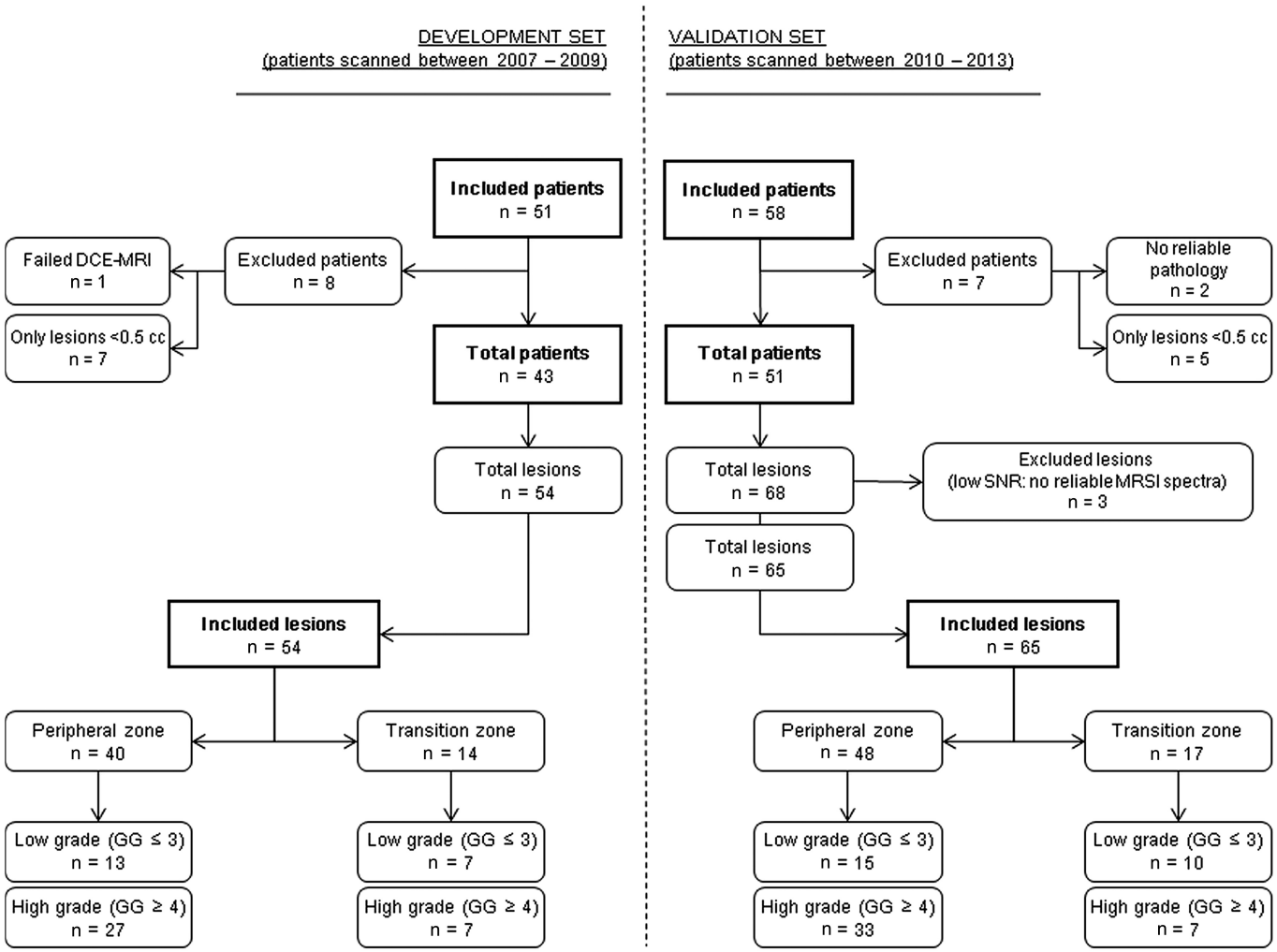

FIGURE 1. Flow diagram of inclusion and exclusion criteria and classification of patient subcohorts.

Data Acquisition

All imaging was performed on a 3-T whole-body system (Magnetom Trio; Siemens, Erlangen, Germany). Between 2007 and 2009, an endorectal coil (Medrad Inc, Pittsburgh, PA) filled with approximately 40 mL of perfluorocarbon and a pelvic phased-array coil were used for signal reception. Between 2010 and 2013, a pelvic phased-array coil, either alone or in combination with the endorectal coil, was used for signal reception. Peristalsis was suppressed with an intramuscular injection of 1 mg glucagon (GlucaGen; Nordisk, Gentofte, Denmark) and 20 mg butylscopolaminebromide (Buscopan; Boehringer-Ingelheim, Ingelheim, Germany), plus an additional intravenous injection of 20 mg Buscopan. High-resolution T2W turbo spin-echo imaging was performed in 3 orthogonal directions. Subsequently, DWI, 3-dimensional MRSI, and DCE-MRI were acquired (Table 1), altogether well within 1 hour.

Histopathologic Analysis

Immediately after the surgery, the prostatectomy specimen was processed according to a clinical protocol. After inking of the surface and fixation with formalin, the prostate was sliced with similar angulation with respect to the rectal wall surface as the slices of the MRI (ie, perpendicular to the rectal wall surface). Subsequently, 1 expert pathologist with over 20 years of experience in urological pathology (C.A.H.V.D.K.) indicated all cancer lesions on photographed slices of the serially sectioned prostate, and a Gleason score was provided for each lesion.[20] Prostate cancer was categorized into aggressiveness classes based on the Gleason growth pattern (GG): low-grade with only GG 3 or less and high-grade with any GG 4 or more. Lesions were classified as peripheral zone (PZ) or transition zone (TZ) cancer.

Magnetic Resonance Imaging Analysis

Parameter maps of the functional techniques were calculated in each patient. In case of misalignment to T2WI, manual registration of the functional techniques onto T2WI was performed by using an in-house developed software tool. For MRSI, parameters of interest were the maximum choline + spermine + creatine over citrate ratio (CSC/C) and the maximum choline over spermine + creatine ratio (C/SC).[21] From DWI, the apparent diffusion coefficient (ADC) map was calculated and used as parameter. For DCE-MRI, descriptive parameters wash-in (slope of the wash-in phase) and washout (slope of the late-wash phase) of the dynamic contrast-enhancement curve were used based on a simplified model as described previously.[22]

Development Set: Determining the Optimal Combination of Parameters

For the development set, cancer lesions were indicated by a radiologist (T.H.) on T2WI based on the prostatectomy specimens and

TABLE 1. Imaging Parameters

Sequence	TR, ms	TE, ms	In-Plane Resolution, mm	Slice/Partition Thickness
Pelvic phased-array coil + endorectal coil (2007–2009)				
T2w axial	3030–5460	84–116	0.4 × 0.4	3
T2w sagittal	3360–5710	98–125	0.5 × 0.5	3
T2w coronal	2400–4290	98–127	0.5 × 0.5	3
DWI	2300–4100	81–96	1.5 × 1.5	3
3D MRSI	750	145	Nominal voxel size, 5 × 5 × 5 or 6 × 6 × 6 mm spherical; voxel size, 0.37/0.64 cm^3	
3D DCE-MRI	2.4–2.9	1.35–1.51	1.5 × 1.5/1.8 × 1.8	3–4
Pelvic phased-array coil + endorectal coil (2010–2013)				
T2w axial	4060–5860	99	0.4 × 0.4	3
T2w sagittal	4290–5020	98	0.5 × 0.5	3
T2w coronal	3590–3910	98	0.5 × 0.5	3
DWI	2600–3000	70–90	1.5 × 1.5/2.0 × 2.0	3
3D MRSI	750	145	Nominal voxel size, 5 × 5 × 5 or 6 × 6 × 6 mm; spherical voxel size, 0.37/0.64 cm^3	
3D DCE-MRI	2.1	1.4	1.5 × 1.5	3–4
Pelvic phased-array coil only (2010–2013)				
T2w axial	4000	101	0.6 × 0.6	3
T2w sagittal	4000	101	0.6 × 0.6	3
T2w coronal	4000	101	0.6 × 0.6	3
DWI	3100	59	2.2 × 1.6	3.6
3D MRSI	750	145	Nominal voxel size, 7 × 7 × 7 mm; spherical voxel size, 1.0 cm^3	
3D DCE-MRI	3.85	1.42	1.6 × 1.6	3.6

Slight differences in parameters were due to a clinical protocol change during the study or whether an endorectal coil was used or not. DWI was recorded with *b* values of 50, 500, and 800 or 100, 400, and 800, depending on the protocol used. An ADC map was calculated automatically by the scanner. DCE-MRI was acquired before, during, and after a 15-mL intravenous bolus injection of gadolinium chelate (Dotarem; Guerbet, France), which was administered with a power injector (Spectris Solaris; Medrad Inc, Indianola, PA) and followed by a 20 mL saline flush. Temporal resolution of 3 seconds (2007–2009) and 4.2 seconds (2010–2013) with total acquisition time of 5 minutes. Nominal and spherical voxel size before and after apodization with the Hanning function.

TR indicates repetition time; TE, echo time; T2w, T2-weighted; DWI, diffusion-weighted imaging; 3D, 3-dimensional; MRSI, magnetic resonance spectroscopic imaging; DCE-MRI, dynamic contrast-enhanced magnetic resonance imaging; ADC, apparent diffusion coefficient.

blinded to any functional imaging parameter. Anatomical landmarks were used as reference when registering pathology slices to the MRI. The size and grid position of individual spectroscopy voxels was used as a region of interest (ROI) because MRSI was the technique with the lowest spatial resolution. Multiple ROIs were drawn to cover each entire tumor lesion (Fig. 2, A–C). Only lesions with a size of 0.5 cm^3 or larger were taken into account.

Subsequently, the ROIs that were drawn on the T2WI were transferred onto the DWI and DCE-MRI parameter images. Because these images had a higher spatial resolution than MRSI, ROIs comprised many voxels in these images, allowing an automated calculation of percentile values for these parameters per ROI. Percentile values of the parameters of functional imaging data were extracted for each ROI per cancer lesion. To account for possible heterogeneity of PCa, for each parameter, the most deviating ROI in each lesion was chosen as representative for that lesion: the maximum CSC/C and C/SC were used from MRSI, the value of the ROI with the lowest 25th percentile of the ADC (ADC25) map was used from DWI, and for DCE-MRI, the values of the ROI with the highest 75th percentile of the wash-in gradient (WI75) and of the ROI with the lowest 25th percentile of the washout gradient (WO25) were used. The choice for these parameters was based on previous studies illustrating their potential to correlate with PCa aggressiveness.[16,18]

Logistic regression modeling (LRM) was used to find the optimal combination of parameters for discriminating low-grade from high-grade PCa. This was done using the stepwise backward elimination approach, by eliminating the parameter with the lowest contributing value (ie, lowest Wald statistic) to the model. Logistic regression modeling models were evaluated using receiver operating characteristic (ROC) curve analysis, using the area under the ROC curve (AUC) as a figure of merit. Peripheral zone and TZ were analyzed separately.

Validation Set: Model Evaluation

The performance of the LRM models was evaluated in the validation set. First, PCa was indicated by a radiologist (E.K.V.) on T2WI in the same way as for the development set, based on the prostatectomy specimens and blinded to any functional imaging parameter and Gleason score. Second, after the indication of the tumor lesions on T2WI, the ROIs were transferred onto the functional imaging data. Subsequently, functional imaging parameters were extracted from each ROI per cancer lesion. Again, for each lesion, the ROIs with the most aberrant value per parameter (ie, per lesion, the maximum CSC/C and C/SC, the lowest ADC25 and WO25, and the highest WI75) were used for analysis.

With the use of the models built in the development set, each lesion was given a probability (*P*) between 0 and 1 of being a high-grade cancer based on their parameter values. To test this model, cutoff point near 0.50 with a relatively high sensitivity (88%) on the ROC curve was chosen to separate high-grade from low-grade cancer, and the corresponding probability value *P* was determined. Cancer lesions in the validation set with an outcome *P* of the LRM below the selected cutoff value were considered low grade and above this cutoff value as high grade. One ROC curve was made, regardless of the zonal origin, to evaluate the discriminating performance in the validation setting.

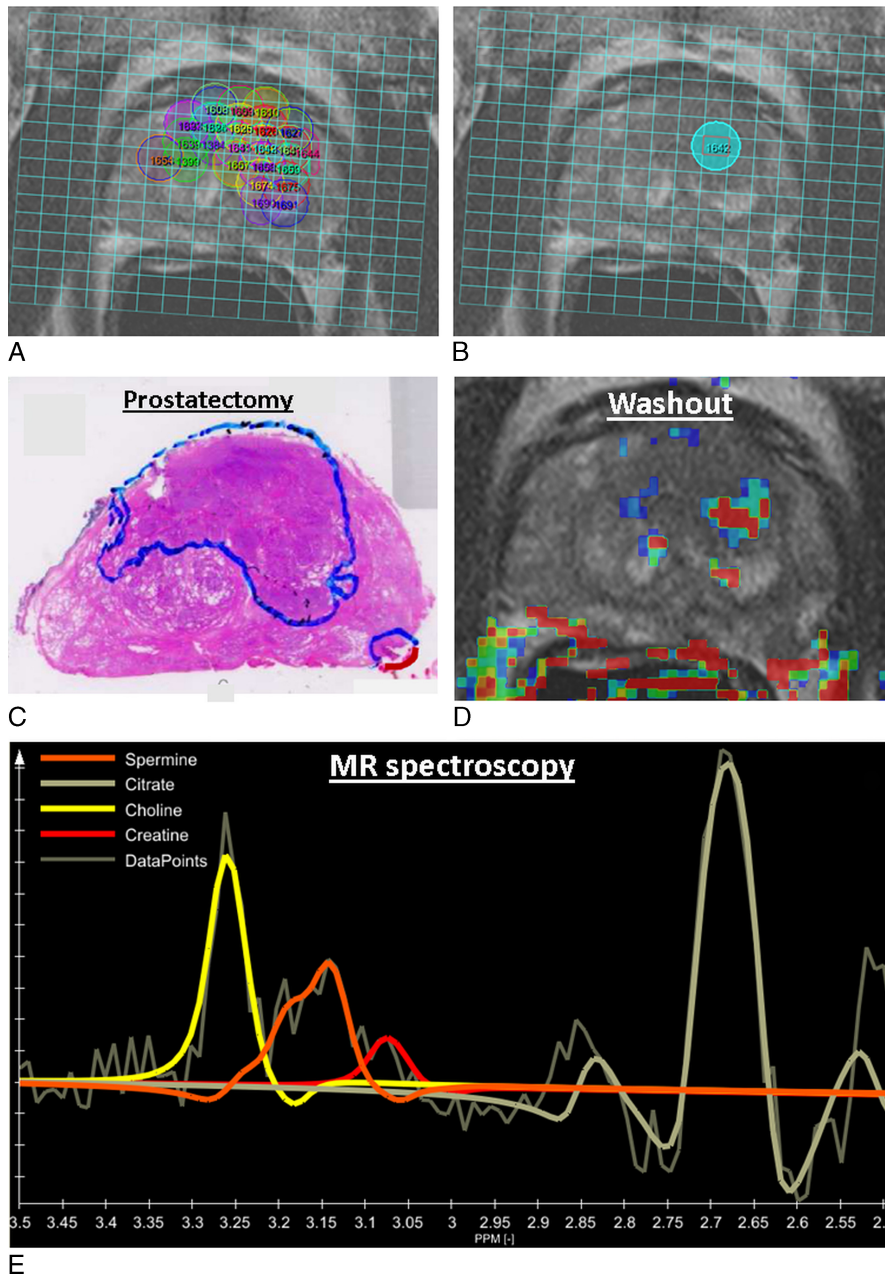

FIGURE 2. Example of a 59-year-old patient with a high-grade PCa lesion (GG ≥4) in the transition zone. A, Annotation of the cancer lesion on axial T2-weighted imaging, with multiple regions of interest (ROIs) covering the entire cancer area. B, One ROI with the size of a spectroscopy voxel, per cancer lesion, the 1 most aberrant value of each parameter of all ROIs is selected for analysis. C, Corresponding prostatectomy slice with the cancer area (blue outline, indicated by the pathologist). D, the washout overlay shows clear washout in a part of the cancer area. E, Spectrum of the selected ROI from Figure 1B; a high choline peak is visible (yellow line), resulting in a high C/SC ratio. Figure 2 can be viewed online in color at www.investigativeradiology.com.

Statistical analyses were performed using GraphPad Prism v.5.0 (GraphPad Software, San Diego, CA) and IBM SPSS statistics for Windows version 20 (IBM Corp, Armonk, NY).

RESULTS

Eight patients were excluded from the development set because of failed DCE-MRI (n = 1) or because the subjects only had lesions of insignificant size (<0.5 cm^3 according to histopathology; n = 7). Overall, 54 cancer lesions were present in the remaining 43 patients (Fig. 1, Table 2).

In the validation set, 7 patients were excluded because no reliable pathology results were available (n = 2) or subjects only had cancer lesions smaller than 0.5 cm^3 (n = 5). In total, 68 cancer lesions were present in the remaining 51 patients. Three cancer lesions (all within the TZ) were excluded from analysis because of an insufficient signal-to-noise ratio of the MRSI spectra. Finally, 65 cancer lesions were included in the validation set (Fig. 1, Table 2).

TABLE 2. Characteristics of Patients and Tumors

Development Set			**Validation Set**		
No. patients		43		52	
PSA, median (range), mg/mL		7.5 (2.1–41.0)		7.0 (2.5–44.9)	
Age, median (range), y		64 (42–70)		62 (48–70)	
Gleason Score		No. Lesions	Gleason Score		No. Lesions
Peripheral zone					
3 + 3	Low*	11	3 + 3	Low	14
3 + 3 + 4	High	1	3 + 4	High	16
3 + 4	High	9	3 + 4 + 5	High	3
3 + 4 + 5	High	2	3 + 5	High	3
4 + 3	High	9	4 + 3	High	4
4 + 3 + 5	High	1	4 + 3 + 5	High	4
4 + 4	High	1	4 + 4	High	1
4 + 4 + 5	High	1	4 + 5	High	2
4 + 5	High	2			
5 + 3	High	1			
Total		**40**			**48**
Low		13			15
High		27			33
Transition zone					
2 + 3	Low	2	1 + 2	Low	1
3 + 2	Low	3	2 + 3	Low	1
3 + 3	Low	2	3 + 2	Low	3
3 + 4	High	1	3 + 3	Low	5
4 + 2	High	1	2 + 3 + 4	High	1
4 + 3 + 5	High	4	3 + 2 + 4	High	3
4 + 5	High	1	4 + 3	High	1
			4 + 3 + 5	High	2
Total		**14**			**17**
Low		7			10
High		7			7

*Cancers are classified in classes according to their aggressiveness, solely based on the Gleason score. Any Gleason grade 4 or higher was considered as high grade.
PSA indicates prostate-specific antigen.

In the development set, the best discrimination performance in the PZ was achieved using an LRM model containing ADC25 and WO25, giving an AUC of 0.85. Separately, these parameters showed AUCs of 0.82 and 0.81, respectively (Table 3). Adding any other parameters to the model did not contribute to the discriminating performance.

The optimal combination of parameters in the TZ proved to be C/SC and WO25, with an AUC of 0.92. Individually, these parameters separately showed AUCs of 0.83 and 0.80, respectively (Table 3). In contrast to the PZ, ADC25 does not perform well in the TZ with only an AUC of 0.65. No additional value was found when any other parameters were included to the model.

An example of the optimal parameter combination in a high-grade PCa in the TZ is shown in Figure 2.

The validation set showed an AUC of 0.75 for the discrimination between low-grade and high-grade PCa, with the different combination of parameters for each zone as described previously. A selected cutoff value on the ROC curve with a sensitivity of 88% and corresponding specificity of 52% ($P > 0.435$) resulted in 18 cancers being classified as low grade and 47 as high grade. With this selected cutoff value, 48 (74%) of 65 cancer lesions were classified correctly, 5 (7%) of 65 were classified as low grade while being high grade (although all with a primary Gleason 3 component; Table 4) according to histopathology (ie, false negative), and 12 (18%) of 65 were classified as high grade while being low grade (ie, false positive; Table 4).

DISCUSSION

The lowest 25th percentile of the ADC + WO25 is the optimal combination for the PZ, and C/SC + WO25 is the optimal combination for the TZ to discriminate between low-grade and high-grade PCa. These combinations showed a higher AUC compared with the use of any single parameter, illustrating the added value for the use of multiple techniques for the assessment of PCa aggressiveness, although the differences between the best performing single parameter and the optimal combination of 2 parameters were not statistically significant. Therefore, larger validation studies are needed to confirm these findings. Adding more techniques to ADC25 + WO25 in the PZ and C/SC + WO25 in the TZ did not increase the discriminating performance at all.

In the validation setting, only few cancer lesions were underestimated (5/65) for their aggressiveness by MRI, and all of these had a primary GG 3 component: 3 + 4 (n = 3) and 3 + 5 (n = 1) originating from the PZ and 1 lesion 3 + 2 with a tertiary 4 component (n = 1, TZ). Although some authors argue that a Gleason score of 3 + 4 could be considered as low-risk disease in specific cases,[23] we decided to consider any secondary or tertiary 4 or 5 component as high grade because

TABLE 3. AUC for Discriminating Between Low-Grade and High-Grade PCa Lesions in the Development Set

	PZ	TZ
Individual parameters		
ADC25	0.82*	0.65
WO25	0.81	0.80
WI75	0.77	0.63
CSC/C	0.74	0.71
C/SC	0.69	0.83†
Combination PZ		
ADC25 + WO25 + WI75 + C/SC + CSC/C	0.85	—
ADC25 + WO25 + WI75 + C/SC	0.85	—
ADC25 + WO25 + WI75	0.85	—
ADC25 + WO25	0.85*	—
Combination TZ		
WO25 + C/SC + WI75 + ADC25 + CSC/C	—	0.92
WO25 + C/SC + WI75 + ADC25	—	0.92
WO25 + C/SC + WI75	—	0.92
WO25 + C/SC	—	0.92†

For the combination, parameters were excluded by using the backward elimination approach of the logistic regression model; in each step, the parameter with the least contributing value to the model was excluded.

*†Difference between AUC of the ROC curves not statistically significant ($P > 0.05$).

AUC indicates area under the receiver operating characteristic curve; PCa, prostate cancer; PZ, peripheral zone; TZ, transition zone; ADC25, lowest 25th percentile of the apparent diffusion coefficient; WO25, lowest 25th percentile of the washout gradient; WI75, highest 75th percentile of the wash-in gradient; CSC/C, choline + spermine + creatine over citrate ratio; C/SC, choline over spermine + creatine ratio; ROC, receiver operating characteristic.

of our methodology (ie, using the ROI with the most aberrant value for analysis and with that, accounting for heterogeneity of PCa or a possible hot spot in the tumor lesion). Perhaps a percentage or volume of GG 4 component within the tumor, to be indicated by the pathologist, could help in this decision. Future work is warranted to correlate mpMRI with an even more meticulous analysis of the exact amount of Gleason 4 component in a cancer lesion. A higher number of cancer lesions (12/65) were predicted more aggressive than the actual Gleason score. In the PZ (n = 8), 7 of these cancers had a Gleason score of 3 + 3, and 1 lesion had a Gleason score of 3 + 2. In the TZ (n = 4), 2 of these cancers had a Gleason score of 3 + 3 and 2 were 3 + 2. Most of these cancers are not aggressive according to Gleason score but may be significant in terms of size.[24,25] However, size was not included in the model as a predictive factor because we only aimed to focus on assessment of aggressiveness according to Gleason score. In clinical practice, volume should be incorporated in the decision-making process for any treatment. In addition, the number of TZ lesions is relatively low. Although the outcome is very promising for the TZ, these results should be interpreted with caution. Future studies with a larger number of subjects are needed to confirm these preliminary results.

In our study setting, it was a deliberate decision to analyze only histologically proven cancer lesions because we aimed to focus on validation of mpMRI for aggressiveness solely, and thus no detection performance or reader study was carried out. To discriminate between low-grade and high-grade PCa in the validation setting, we selected a cutoff value with a relatively high sensitivity to ensure that fewer subjects would be classified false negative. Any cutoff point on the ROC curve could have been chosen; however, the rationale for selecting this point is that one needs to reduce the probability of underestimation of aggressiveness while at the same time definite highly aggressive PCa needs to be recognized reliably. As a next step, both the detection and characterization of PCa could be evaluated by incorporating our findings in this complete evaluation package, followed by a reader study to confirm its true prognostic value.

Over the last years, active surveillance has gained more interest for patients with low-risk PCa,[26,27] but concerns remain that the patient's tumor is actually more aggressive than estimated on the basis of current diagnostic tools such as prostate-specific antigen or systematic transrectal ultrasound biopsies.[28] A recent study by Turkbey et al[29] showed that mpMRI provides useful additional information to existing clinical scoring systems, and it improves the assignment to either active treatment or active surveillance; however, the patient cohort and methods in that study are very different from ours (eg, in that study, only patients who met the criteria for active surveillance based on clinical scoring systems were included; MR parameters were evaluated on a suspicion-level basis; and no correlations of the individual parameters to Gleason scores were reported). Many other studies have been performed regarding mpMRI for PCa. Most of these studies focused on the detection of PCa rather than the assessment of aggressiveness and used transrectal ultrasound biopsies as a reference standard or did not evaluate the full combination of functional MRI techniques.[1,2,6,30–33] To the best of our knowledge, this is the first study that evaluated all 3 functional techniques together, with a solid reference standard to find the optimal combination of parameters for the assessment of PCa aggressiveness, for the PZ and TZ separately.

TABLE 4. Classification of Aggressiveness in Low-Grade and High-Grade for the Validation Set Based on the Models Built Using the Development Set

	mpMRI	Histopathology Results		
Zone	Aggr	Aggr	GG	Vol, cm^3
Correct classification				
PZ (n = 36)	Low (n = 7)	Low	GG ≤3	
	High (n = 29)	High	GG ≥4	
TZ (n = 12)	Low (n = 6)	Low	GG ≤3	
	High (n = 6)	High	GG ≥4	
Incorrect classification				
PZ (n = 12)	Low (n = 4)	High	3 + 4	0.6
			3 + 4	1.3
			3 + 4	2.6
			3 + 5	1.1
	High (n = 8)	Low	3 + 3	11.7
			3 + 3	0.5
			3 + 3	2.1
			3 + 3	5.3
			3 + 3	0.6
			3 + 3	3.4
			3 + 3	1.0
			3 + 3	1.0
TZ (n = 5)	Low (n = 1)	High	3 + 2 (+4)	10.0
	High (n = 4)	Low	3 + 3	2.5
			3 + 3	0.7
			3 + 2	1.0
			3 + 2	1.3

mpMRI indicates multiparametric magnetic resonance imaging; Aggr, aggressiveness level; GG, Gleason grade; Vol, volume; PZ, peripheral zone; TZ, transition zone.

The reason for incorporating spermine into the metabolite ratios is that this peak can overlap with the creatine peak in the spectra. Neglecting this peak can lead to overestimation of the choline or creatine peak, and thus lead to an incorrect metabolite ratio. The rationale for using only semiquantitative DCE-MRI parameters is that they are relatively easy to calculate in contrast to pharmacokinetic parameters. Moreover, pharmacokinetic parameters are not suitable for widespread application in different institutes with different acquisition protocols because of the fact that numerous approaches for modeling exist and calibration by using an arterial input function can be done in multiple ways. Implementation and interpretation of both MRSI and DCE-MRI require experience. Incorporation in clinical practice may thus be reserved for specialized institutions or require robust standardized automation for widespread clinical use. Our results indicate that both techniques show potential in the assessment of PCa aggressiveness, and it therefore may be worthwhile to indeed invest in standardization and automation of both MRSI and DCE-MRI for an mpMRI approach to characterize PCa.

Our results could be of important clinical value. We found that different combinations of techniques should be used for the assessment of PCa aggressiveness in the PZ and TZ. Although ADC usually performs well for the detection of PCa regardless of the location within the prostate, we have shown that ADC is not of any value for predicting the aggressiveness of cancer lesions in the TZ, and these results are in line with previous reports.[34,35] In contrast, DCE-MRI regularly shows false positives in a detection setting, whereas our results show that WO25 is useful for the assessment of aggressiveness of an already detected and localized cancer lesion, when combined with ADC in the PZ and C/SC in the TZ. In the future, this can be relevant for follow-up of histopathologically proven PCa. The combination of techniques in mpMRI offers a noninvasive imaging tool as a method for the assessment of PCa aggressiveness and may provide useful information to incorporate in nomograms or in the decision-making process for recognizing those patients who need definite treatment or for selecting patients suitable to stay on active surveillance and thus preventing overtreatment of PCa.

In conclusion, mpMRI is a useful tool for the discrimination between low-grade and high-grade PCa and performs better than any single individual functional parameter in both PZ and TZ. For the PZ, the proposed optimal combination of parameters is the 25th percentile of ADC derived from DWI and the 25th percentile of washout derived from DCE-MRI. For the TZ, washout may be combined with the C/SC acquired by MRSI, and ADC is not of any value. Adding any other technique does not increase the discriminating performance at all.

ACKNOWLEDGMENT

The authors thank P. Peer, PhD, for the statistical consultation.

REFERENCES

1. Turkbey B, Pinto PA, Mani H, et al. Prostate cancer: value of multiparametric MR imaging at 3 T for detection—histopathologic correlation. *Radiology*. 2010;255:89–99.
2. Isebaert S, Van den Bergh L, Haustermans K, et al. Multiparametric MRI for prostate cancer localization in correlation to whole-mount histopathology. *J Magn Reson Imaging*. 2012;37:1392–1401.
3. Hoeks CMA, Hambrock T, Yakar D, et al. Transition zone prostate cancer: detection and localization with 3-T multiparametric MR imaging. *Radiology*. 2013;266:207–217.
4. Panebianco V, Sciarra A, Marcantonio A, et al. Conventional imaging and multiparametric magnetic resonance (MRI, MRS, DWI, MRP) in the diagnosis of prostate cancer. *Q J Nucl Med Mol Imaging*. 2012;56:331–342.
5. Busetto GM, De Berardinis E, Sciarra A, et al. Prostate cancer gene 3 and multiparametric magnetic resonance can reduce unnecessary biopsies: decision curve analysis to evaluate predictive models. *Urology*. 2013;82:1355–1360.
6. Vaché T, Bratan F, Mège-Lechevallier F, et al. Characterization of prostate lesions as benign or malignant at multiparametric MR imaging: comparison of three scoring systems in patients treated with radical prostatectomy. *Radiology*. 2014;272:446–455.
7. Godtman RA, Holmberg E, Khatami A, et al. Outcome following active surveillance of men with screen-detected prostate cancer. Results from the Göteborg randomised population-based prostate cancer screening trial. *Eur Urol*. 2013;63:101–107.
8. Klotz L. Strengthening evidence for active surveillance for prostate cancer. *Eur Urol*. 2013;63:108–110.
9. Pelzer AE, Bektic J, Berger AP, et al. Are transition zone biopsies still necessary to improve prostate cancer detection? Results from the tyrol screening project. *Eur Urol*. 2005;48:916–921; discussion 921.
10. Kvåle R, Møller B, Wahlqvist R, et al. Concordance between Gleason scores of needle biopsies and radical prostatectomy specimens: a population-based study. *BJU Int*. 2009;103:1647–1654.
11. Hoeks CMA, Somford DM, van Oort IM, et al. Value of 3-T multiparametric magnetic resonance imaging and magnetic resonance-guided biopsy for early risk restratification in active surveillance of low-risk prostate cancer: a prospective multicenter cohort study. *Invest Radiol*. 2014;49:165–172.
12. Hambrock T, Hoeks C, Hulsbergen-van de Kaa C, et al. Prospective assessment of prostate cancer aggressiveness using 3-T diffusion-weighted magnetic resonance imaging–guided biopsies versus a systematic 10-core transrectal ultrasound prostate biopsy cohort. *Eur Urol*. 2012;61:177–184.
13. Vargas HA, Akin O, Franiel T, et al. Diffusion-weighted endorectal MR imaging at 3 T for prostate cancer: tumor detection and assessment of aggressiveness. *Radiology*. 2011;259:775–784.
14. Donati OF, Mazaheri Y, Afaq A, et al. Prostate cancer aggressiveness: assessment with whole-lesion histogram analysis of the apparent diffusion coefficient. *Radiology*. 2014;271:143–152.
15. Rosenkrantz AB, Sigmund EE, Johnson G, et al. Prostate cancer: feasibility and preliminary experience of a diffusional kurtosis model for detection and assessment of aggressiveness of peripheral zone cancer. *Radiology*. 2012;264:126–135.
16. Vos EK, Litjens GJ, Kobus T, et al. Assessment of prostate cancer aggressiveness using dynamic contrast-enhanced magnetic resonance imaging at 3 T. *Eur Urol*. 2013;63:448–455.
17. Kobus T, Hambrock T, Hulsbergen-van de Kaa CA, et al. In vivo assessment of prostate cancer aggressiveness using magnetic resonance spectroscopic imaging at 3 T with an endorectal coil. *Eur Urol*. 2011;60:1074–1080.
18. Kobus T, Vos PC, Hambrock T, et al. Prostate cancer aggressiveness: in vivo assessment of MR spectroscopy and diffusion-weighted imaging at 3 T. *Radiology*. 2012;265:457–467.
19. Nagarajan R, Margolis D, Raman S, et al. MR spectroscopic imaging and diffusion-weighted imaging of prostate cancer with Gleason scores. *J Magn Reson Imaging*. 2012;36:697–703.
20. Epstein JI, Allsbrook WC Jr, Amin MB, et al. The 2005 International Society of Urological Pathology (ISUP) Consensus Conference on Gleason grading of prostatic carcinoma. *Am J Surg Pathol*. 2005;29:1228–1242.
21. Kobus T, Wright AJ, Weiland E, et al. Metabolite ratios in 1 H MR spectroscopic imaging of the prostate. *Magn Reson Med*. 2014. [Epub ahead of print].
22. Huisman HJ, Engelbrecht MR, Barentsz JO. Accurate estimation of pharmacokinetic contrast-enhanced dynamic MRI parameters of the prostate. *J Magn Reson Imaging*. 2001;13:607–614.
23. Van den Bergh RC, Roemeling S, Roobol MJ, et al. Gleason score 7 screen-detected prostate cancers initially managed expectantly: outcomes in 50 men. *BJU Int*. 2009;103:1472–1477.
24. Sebo TJ, Bock BJ, Cheville JC, et al. The percent of cores positive for cancer in prostate needle biopsy specimens is strongly predictive of tumor stage and volume at radical prostatectomy. *J Urol*. 2000;163:174–178.
25. Kryvenko ON, Carter HB, Trock BJ, et al. Biopsy criteria for determining appropriateness for active surveillance in the modern era. *Urology*. 2014;83:869–874.
26. Bul M, van den Bergh RC, Rannikko A, et al. Predictors of unfavourable repeat biopsy results in men participating in a prospective active surveillance program. *Eur Urol*. 2012;61:370–377.
27. Bul M, Zhu X, Valdagni R, et al. Active surveillance for low-risk prostate cancer worldwide: the PRIAS study. *Eur Urol*. 2013;63:597–603.
28. Shaw GL, Thomas BC, Dawson SN, et al. Identification of pathologically insignificant prostate cancer is not accurate in unscreened men. *Br J Cancer*. 2014;110:2405–2411.
29. Turkbey B, Mani H, Aras O, et al. Prostate cancer: can multiparametric MR imaging help identify patients who are candidates for active surveillance? *Radiology*. 2013;268:144–152.

30. Peng Y, Jiang Y, Yang C, et al. Quantitative analysis of multiparametric prostate MR images: differentiation between prostate cancer and normal tissue and correlation with Gleason score—a computer-aided diagnosis development study. *Radiology*. 2013;267:787–796.
31. Peng Y, Jiang Y, Antic T, et al. Validation of quantitative analysis of multiparametric prostate MR images for prostate cancer detection and aggressiveness assessment: a cross-imager study. *Radiology*. 2014;271:461–471.
32. Arumainayagam N, Ahmed HU, Moore CM, et al. Multiparametric MR imaging for detection of clinically significant prostate cancer: a validation cohort study with transperineal template prostate mapping as the reference standard. *Radiology*. 2013;268:761–769.
33. Bonekamp D, Bonekamp S, Mullins JK, et al. Multiparametric magnetic resonance imaging characterization of prostate lesions in the active surveillance population: incremental value of magnetic resonance imaging for prediction of disease reclassification. *J Comput Assist Tomogr*. 2013;37:948–956.
34. Hoeks CMA, Vos EK, Bomers JG, et al. Diffusion-weighted magnetic resonance imaging in the prostate transition zone: histopathological validation using magnetic resonance-guided biopsy specimens. *Invest Radiol*. 2013;48:693–701.
35. Verma S, Rajesh A, Morales H, et al. Assessment of aggressiveness of prostate cancer: correlation of apparent diffusion coefficient with histologic grade after radical prostatectomy. *AJR Am J Roentgenol*. 2011;196:374–381.